The 12th Iranian Aerospace Society Conference
Amir Kabir University of Technology

AERO2013-18514

Numerical Simulation of 3-D Cavitation behind a Disk Cavitator Using OpenFOAM

Amin Rahimi, Ehsan Roohi, Mohammad Javad Maghrebi

Department of Mechanical Engineering, Ferdowsi University of Mashhad,
Mashhad, Iran, P.O.Box: 91775-1111

Abstract

In this paper simulation of cavitating flow over a disk cavitator is reported using computational fluid dynamics (CFD) technique. To apply the cavitation model, the flow has been considered as a single fluid, two-phase mixture. A transport equation model for the local volume fraction of vapor is solved and a finite rate mass transfer model is used for the vaporization and condensation processes based on the Kunz model. The volume of fluid (VOF) method is applied to track the interface of liquid and vapor phases. Our simulation is performed using a two phase solver available in the framework of the OpenFOAM package, namely "interPhaseChangeFoam". The solver is based on finite volume method. Two different turbulence model, i.e., k-ω SST and large eddy simulation (LES) are employed. Simulation is performed for the supercavitation regime. The results of our simulation are compared with the experimental data and analytical expressions and suitable accuracy has been investigated.

Keywords: *Disk cavitator- LES turbulence model- mass transfer model- VOF.*

Introduction

Formation of vapor bubbles within a liquid when its pressure is less than the saturated vapor pressure is called cavitation. The cavitation usually appears over marine vehicles. For efficiency reasons, some marine vehicles usually needs to be operated in cavitating conditions but one still needs to avoid the negative effects of cavitation such as vibrations, noise and erosion [1].

The numerical simulation of cavitation phenomenon does however include many complications from modeling and computational point of views. Free surface reconstruction is one of the challenges of cavitation modeling [2]. Phase change from liquid to water is difficult to model on a macroscopic level and the cavitation dynamics is governed by medium to small flow scales, both in time and space, necessitating large computational grids and small time steps. According to the literature, there is different cavitation mass transfer models such as Sauer [3], Kunz et al [4] and Merkle et al [5].

Previous investigations on cavitation considered various numerical frameworks, i.e., Passandideh-Fard and Roohi [6] performed transient 2D/axisymmetric simulations of cavitating flows assuming laminar fluid flow. Nouri et al. [7] used a finite volume method to simulate cavitation over a disk, using the Kunz cavitation model and considering large eddy viscosity as a turbulence model. Baradaran Fard and Nikseresht [8] simulated an unsteady 3D cavitating flows over axisymmetric cavitators. For implementation of turbulent flow, the shear stress transport, $\kappa-\omega$ model was used. Shang et al [9] validated the numerical simulations of cavitating sphere with the experimental data. Zahiri et al [10] used LES turbulence to investigate cavitating flows over airfoils using the OpenFOAM package.

In this research, we validated the ability of an open source package, that is, OpenFOAM package to simulate supercavitation flow behind a disk whose experimental/analytical data is available [1]. Volume of fluid (VOF) technique is applied to track the interface of liquid and vapor phases [2]. VOF model used in the OpenFOAM considers the effect of the surface tension force over the free surface. In the current work, we use both of LES and $\kappa-\omega$ SST turbulence models to simulate cavitating flows behind a disk.

Governing Equations

The vapor-liquid flow described by a single-fluid model is treated as a homogeneous bubble-liquid mixture, so only one set of equations is needed to simulate cavitating flows. Thus, starting from the incompressible Navier-Stokes (NS) equations:

$$\partial_t \rho + \nabla.(\rho v) = 0$$
$$\partial_t (\rho v) + \nabla.(\rho v \times v) = -\nabla p + \nabla.s, \qquad (1)$$

Eqs. (1) is the governing continuity and momentum equations for a classical RANS and homogeneous mixture multiphase flow. Where v is the velocity, p is the pressure, $s = 2\mu D$ is the viscous stress tensor, where the rate-of-strain tensor is expressed as

$$D = \frac{1}{2}\left(\nabla v + \nabla v^T\right) \qquad (2)$$

Where μ is the viscosity.

Turbulence model

1. LES Model

Large eddy simulation (LES) is based on computing the large, energy-containing structures that are resolved on the computational grid, whereas the

1. MSc student
2. Assistant Professor, Tel/Fax: 0511-8763304, email: e.roohi@um.ac.ir (corresponding author)
3. Associate professor

smaller, more isotropic, sub-grid structures are modeled. In contrast to RANS approaches, which are based on solving for an ensemble average of the flow properties, LES naturally and consistently allows for medium to small scale, transient flow structures. When simulating unsteady, cavitating flows, it is an important property in order to be able to capture the mechanisms governing the dynamics of the formation and shedding of the cavity [11-12]. The LES equations are theoretically derived, following e.g. Sagaut [13] from Eq. (1). In ordinary LES, all variables, i.e., *f*, are split into grid scale (GS) and sub grid scale (SGS) components, $f = \bar{f} + f'$, where $\bar{f} = G * f$ is the GS component, $G = G(X, \Delta)$ is the filter function, and $\Delta = \Delta(\mathbf{x})$ is the filter width. The LES equations result from convolving the NS with *G*, viz,

$$\begin{aligned} &\partial_t\left(\bar{\rho}\bar{v}\right) + \nabla.\left(\bar{\rho}\bar{v}\times\bar{v}\right) = -\nabla\bar{p} + \nabla.\left(\bar{s} - B\right), \\ &\partial_t\rho + \nabla.\left(\bar{\rho}\bar{v}\right) = 0 \end{aligned} \tag{3}$$

Where over-bar denotes filtered quantity. Equation (3) introduces one new term when compared to the unfiltered Eq. (1): the unresolved transport term *B*, which is the sub grid stress tensor. Following Bensow and Fureby [14], *B* can be exactly decomposed as

$$\boldsymbol{B} = \rho.\left(\overline{\bar{v}\times\bar{v}} - \bar{\bar{v}}\times\bar{\bar{v}} + \widetilde{B}\right) \tag{4}$$

, Where now only $\widetilde{B}$ needs to be modeled. The most common subgrid modeling approaches utilizes an eddy or subgrid viscosity, ν_{SGS}, similar to the turbulent viscosity approach in RANS, where ν_{SGS} can be computed in a wide variety of methods. In eddy-viscosity models often,

$$B = \frac{2}{3}\bar{\rho}kI - 2\mu k\,\tilde{D}_D \tag{5}$$

Where *k* is the SGS kinetic energy, $\bar{\rho}$ the SGS eddy viscosity, and $\tilde{D}_D$ the SGS eddy diffusivity. In the current study, sub-grid scale terms are modeled using "one equation eddy viscosity" model. In order to obtain *k,* one-equation eddy-viscosity model (OEEVM) uses the following equation:

$$\partial\left(\bar{\rho}k\right) + \nabla.\left(\bar{\rho}k\,\tilde{v}\right) = -B.\tilde{D} + \nabla.(\mu\nabla\mathrm{k}) + \bar{\rho}\varepsilon \tag{6}$$

, where

$$\varepsilon = c_\varepsilon k^{3/2} / \Delta \tag{7}$$

And

$$\mu_\mathrm{k} = c_k\bar{\rho}\Delta\sqrt{k} \tag{8}$$

2. k-ω SST model

In addition to LES, the shear stress Transport (SST) $\kappa-\omega$ model is utilized for turbulence modeling. The $\kappa-\omega$ SST model was developed be Menter [15] to effectively blend the robust and accurate formulation of the $\kappa-\omega$ model in the near-wall region with the free-stream independence of the $\kappa-\varepsilon$ model in the far field. To achieve this, the $\kappa-\varepsilon$ model is converted into a $\kappa-\omega$ formulation. The governing equations are as follow:

Turbulence Kinetic Energy:

$$\begin{aligned} &\frac{\partial}{\partial t}(\rho k) + \frac{\partial}{\partial x_j}(\rho k u_j) = \frac{\partial}{\partial x_j}\left(\left(\mu + \frac{\mu_t}{\sigma_{k3}}\right)\frac{\partial k}{\partial x_j}\right) \\ &+\tau_{ij}\frac{\partial u_i}{\partial x_j} - \beta^*\rho k\omega. \end{aligned} \tag{9}$$

Specific dissipation rate:

$$\begin{aligned} &\rho\frac{\partial\omega}{\partial t} + \rho u_j\frac{\partial\omega}{\partial x_j} = \frac{\partial}{\partial x_j}\left(\left(\mu + \frac{\mu_t}{\sigma_{\omega 3}}\right)\frac{\partial\omega}{\partial x_j}\right) \\ &+\frac{\omega}{k}\left(\alpha_3\tau_{ij}\frac{\partial u_i}{\partial x_j} - \beta_3\rho k\omega\right) \\ &+(1-F_1)2\rho\frac{1}{\omega\sigma_{\omega 2}}\frac{\partial k}{\partial x_j}\frac{\partial\omega}{\partial x_j}, \end{aligned} \tag{10}$$

Where the coefficients of the model are a linear combination of the corresponding coefficients of the $\kappa-\omega$ and modified $\kappa-\varepsilon$ models as:

$$\begin{aligned} &\left(\psi = F_1\psi_{k\omega} + \left(1-F_1\right)\psi_{k\varepsilon}\right). \\ &k-\omega: \alpha_1 = 5/9, \beta_1 = 3/40, \sigma_{k1} = 2, \\ &\sigma_{\omega 1} = 2, \beta^* = 9/100, \\ &k-\varepsilon: \alpha_2 = 0.44, \beta_2 = 0.0828, \sigma_{k2} = 1, \\ &\sigma_{\omega 2} = 1/0.856, C_\mu = 0.09. \end{aligned}$$

The model combines the advantages of the Wilcox $\kappa-\omega$ and the Launder-Spalding $\kappa-\varepsilon$ models, but still fails to properly predict the onset and amount of the flow separation from smooth surfaces, due to the over-prediction of the eddy-viscosity (the transport of the turbulence shear stress is not properly taken into account). The proper transport behavior can be obtained by a limiter added to the formulation of the eddy-viscosity:

$$\mu_t = \rho\frac{k}{\max\left(\omega, SF_2\right)}, \tag{11}$$

Where F_2 is blending function, which restricts the limiter to the wall boundary layer, as the underlying assumptions are not correct for free shear flow. S is an invariant measure of the strain rate. The blending

functions F_1 and F_2 are critical to the success of the method.

Multiphase Flow Modeling

To model cavitating flows, the two phases of liquid and vapor need to be specified as well as the phase transition mechanism between them. In this work, we consider a "two-phase mixture" method, which uses a local vapor volume fraction transport equation together with source terms for the mass transfer rate between the two phases due to cavitation.

$$\partial_t \gamma + \nabla.\left(\gamma \bar{v}\right) = \dot{m} \tag{12}$$

The density and viscosity in Eq. (3) are assumed to vary linearly with the vapor fraction,

$$\mu = \gamma\mu_v + (1-\gamma)\mu_l \tag{13}$$

$$\rho = \gamma\rho_v + (1-\gamma)\rho_l \tag{14}$$

In this work, we had employed Kunz models. Kunz et al. [4] proposed a semi-analytical cavitation model as follows:

$$\frac{\partial\gamma}{\partial t} + \vec{\nabla}\cdot(\gamma\bar{v}) = \frac{C_{dest}\rho_v Min(P_l - P_v, 0)\gamma}{\rho_l(0.5\rho_l V_\infty^2)t_\infty} + \frac{C_{prod}(1-\gamma)\gamma^2}{\rho_l t_\infty} \tag{15}$$

, Where C_{dest} and C_{prod} are two empirical constants. Due to condensation, there will be a continuous flow of reentrant liquid jet near the cavity closure which in turn causes small vapor structures to detach from the end of the cavity continuously. To include this phenomenon more effectively, Kunz's model assumes a moderate rate of constant condensation. Kunz's model reconstructs the cavity region quite accurately especially in the closure region o the cavity. Therefore we employed Kunz model in the current simulation.

VOF Model

OpenFOAM uses an improved version of "The Compressive Interface Capturing Scheme for Arbitrary Meshes (CICSAM)" VOF technique, based on Ubbink's work [16]. CICSAM is implemented in OpenFOAM as an explicit scheme and could produce an interface that is almost as sharp as the geometric reconstruction schemes such as PLIC. In CICSAM approach, a supplementary "interface-compression velocity (U_c)" is defined in the vicinity of the interface in such a way that the local flow steepens the gradient of the volume fraction function and the interface resolution is improved. This is incorporated in the conservation equation for volume fraction (γ) in the following form (14):

$$\frac{\partial\gamma}{\partial t} + \nabla.(\gamma\bar{\upsilon}) + \nabla.[\bar{\upsilon}_c\gamma(1-\gamma)] = 0 \tag{16}$$

The last term on the left-hand side of the above equation is known as the artificial compression term and it is non-zero only at the interface. The compression term stands for the role to shrink the phase-inter phase towards a sharper one. The compression term does not bias the solution in any way and only introduces the flow of γ in the direction normal to the interface. In order to ensure this procedure, Weller suggested the compression velocity to be calculated as:

$$\bar{\upsilon}_c = \min[c_\gamma |\bar{\upsilon}|, \max(|\bar{\upsilon}|)]\frac{\nabla\gamma}{|\nabla\gamma|} \tag{17}$$

In other words, the compression velocity is based on the maximum velocity at the interface. The limitation of v_c is achieved through applying the largest value of the velocity in the domain as the worst possible case. The intensity of the compression is controlled by a constant C_γ, i.e., it yields no compression if it is zero, a conservative compression for C_γ=1 and high compression for C_γ>1. Nevertheless, the CICSAM Algorithm is far less costly to apply compared to PLIC. Previous studies showed that OpenFOAM will give accurate results for the interface position on moderate to high resolution meshes.

Solution Algorithm

Since there exists no explicit equation for pressure and therefore de-coupling of pressure from velocity must be avoided. This is done by deriving a discretized pressure equation from the semi-discretized momentum equation, using the continuity restriction of a divergence-free velocity field coming from the equation for mass conservation. The velocity and pressure are coupled through the Pressure Implicit with Splitting of Operators (PISO) algorithm for transient flows of Issa [17]. A summary of the algorithm is presented by Jasak [18] and is more detailed by Rusche [19].

Simulation Set-up

The computational domain and boundary conditions are shown in Fig 1. The disk is placed at the center of water tunnel. The two important non-dimensional numbers used are the Reynolds number (Re) and cavitation number σ. U_∞ is the free stream velocity which is imposed 20 m/s. we have $\sigma = 0.245$ and $Re = 544444$.

Grid Properties

As the disk is not geometrically complex, we used structured quadrilateral meshes. Mesh size near the disk has a key effect on the simulation results. Meshes are refined in both axial and radial directions to get a cavitation shape like the experimental data. There are 790000 cells in the domain. This results in a heavy computational procedure. Fig. 2 illustrates the mesh which is produced around the disk. The distance between disk and outlet is set as 12D in order to prepare a suitable distance between the outlet and cavity region.

Results and Discussions

Figures 3-4 illustrate a 3D view of the cavitating flow over the disk in $\sigma = 0.2$ and $\sigma = 0.245$. The cavity shape has a uniform shape and it is in good agreement with supercavitation condition which has a steady behavior. The contour of volume fraction is illustrated in Fig. 5 and Fig. 6 as a 2D section in z plane at $\sigma = 0.2$ and 0.245 respectively. Fig. 7 and Fig. 8 show the side view and 3D view of cavitation with LES turbulence model at five time steps, respectively. These figures illustrate that cavity grows up step by step and reaches to a fix length at the final step. The figures also show the unsteady nature of the cavitation. Fig. 9 and Fig. 10 illustrate the results of $\kappa - \omega$ SST turbulence model. The figure show that cavitation reached to steady state much sooner in contrast to the LES solution. The cavity thickness at different sections along the cavity is illustrated in Fig.11, which shows that the thickness increases to a maximum and then decreases, and the cavity will be closed. LES turbulence model and $\kappa - \omega$ SST turbulence model are being compared in Fig. 12, LES model shows flow separation near the cavity closure region while the $\kappa - \omega$ SST model predicts a continuous cavity.

Figure 13 shows the formation of re-entrant jets using LES turbulence model. Meanwhile, the $\kappa - \omega$ SST model does not predict this behavior. Typically, cavity lengths increase once the cavitation number decreases see Fig. 14. Figure 15 illustrate the contour of pressure, pressure increases at the front of disk due to flow impact on the wall, i.e., pressure at stagnation point reaches to 200 kPa, but behind the disk, the flow separates at the sharp edge and the resultant drop in pressure creates a vaporous cavity region. A pressure gradient appears at the interface of vapor phase and liquid phase. This id created due to pressure difference between two phases and is normal to the interface. On the other hand, cavity shedding and condensation of cavity bubbles cause a high pressure variation at the end of cavity region. A sharp interface is visible around the cavity domain which is the result of using VOF model.

Three dimensionless parameters are compared from our simulation with those of experiments and analytical relations, see Table 1 and Table 2. For validating the present results, the Richardt's semi-empirical relations are selected as non-dimensional characteristics of the cavity. The related formulas for these characteristics are presented by Eqs. (18)-(20). The cavitation number is the main factor in these in these formulas [20]

$$\frac{L}{d} = \frac{\sigma + 0.008}{\sigma\left(1.7\sigma + 0.066\right)}\left(\frac{d}{D}\right) \tag{18}$$

$$\frac{d}{D} = \left[\frac{C_D}{\sigma\left(1 - 0.132\sigma^{0.5}\right)}\right]^{0.5} \tag{19}$$

$$C_D = C_{D_0}\left(1 + \sigma\right) \tag{20}$$

L/d and D/d are the ratio of cavity length and cavity diameter to the cavitator diameter, respectively. There are good agreement between the numerical and experimental results in both simulated cavitation numbers. The numerical results have a better agreement with the experimental data comparing with the theoretical predictions. Additionally, drag coefficient (C_D) obtained from the pressure distribution over the disk surface has a good accuracy comparing with theoretical and experimental results.

Conclusion

In the present study, a finite volume solver benefiting from the VOF interface capturing method and LES or k-ω SST turbulence model has been employed to capture unsteady supercavitation flow behind a 3-D disk cavitator. The simulation is performed under the framework of OpenFOAM. The Kunz mass transfer model is employed for cavitation modeling. Our simulation shows that combination of VOF and Kunz models has a precise ability to simulate the supercavitation features including cavity shape, closure region and drag coefficient once compared with the experimental data and analytical expressions.

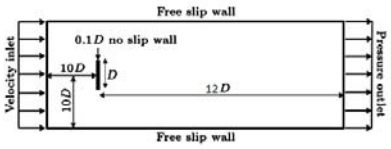

Fig. 1: Computational domain and boundary conditions.

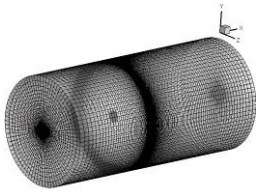

Fig. 2: Mesh generation.

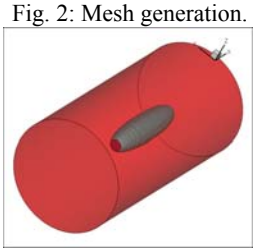

Fig. 3: 3D cavitation behind a disk $\sigma = 0.2$

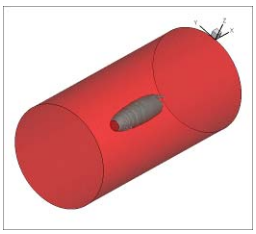

Fig. 4: 3D cavitation behind a disk $\sigma = 0.245$

Fig. 5: Contour of vapor phase (cavity region) for $\sigma = 0.2$

Fig. 6: Contour of vapor phase (cavity region) for $\sigma = 0.245$

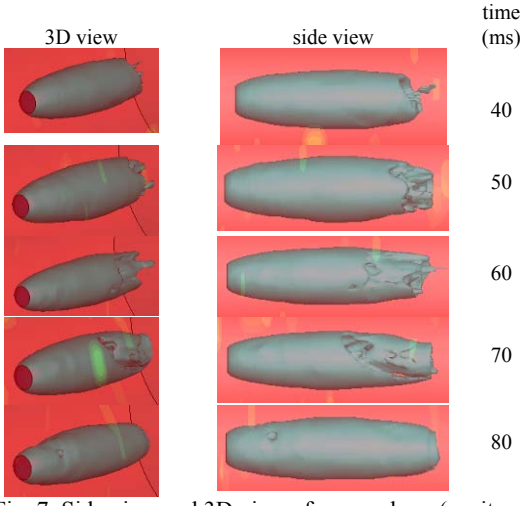

Fig. 7: Side view and 3D view of vapor phase (cavity region) for $\sigma = 0.245$ with LES turbulence model

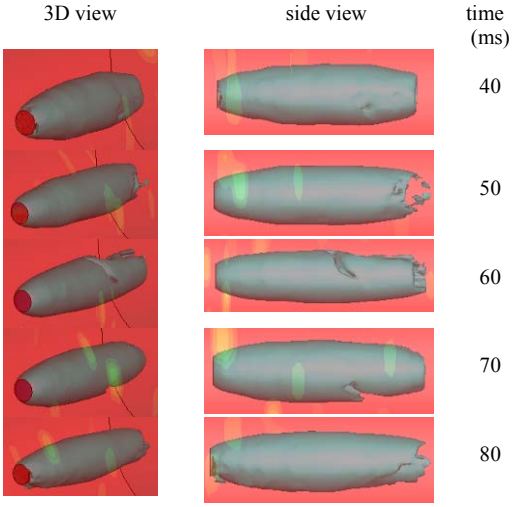

Fig. 8: Side view and 3D view of vapor phase (cavity region) for $\sigma = 0.2$ with LES turbulence model

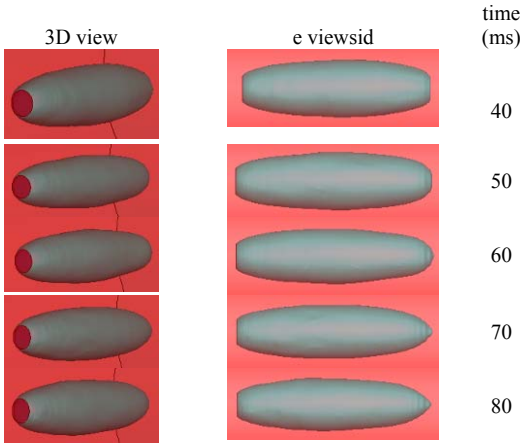

Fig. 9: Side view and 3D view of vapor phase (cavity region) for $\sigma = 0.2$ with $\kappa - \omega$ SST turbulence model

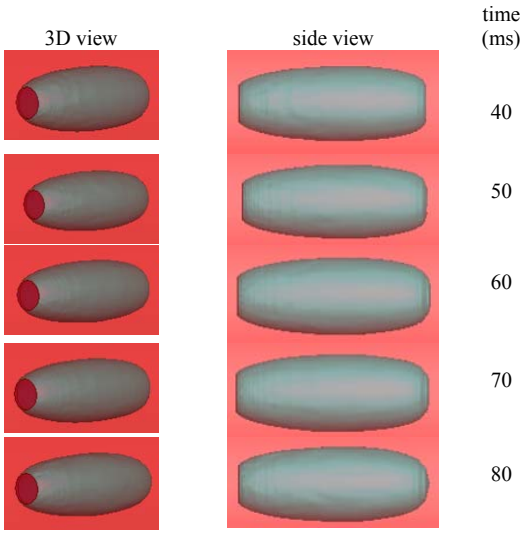

Fig. 10: Side view and 3D view of vapor phase (cavity region) for $\sigma = 0.245$ with $\kappa - \omega$ SST turbulence model

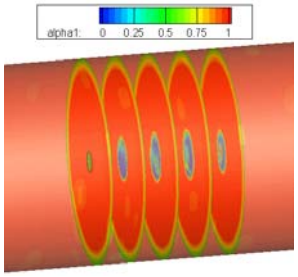

Fig. 11: Section of cavitating flow for $\sigma = 0.245$

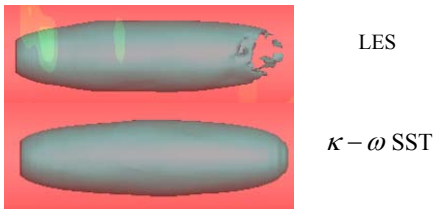

Fig. 12: Comparing the turbulence models effects on the cavity behavior at 50 ms for $\sigma = 0.2$

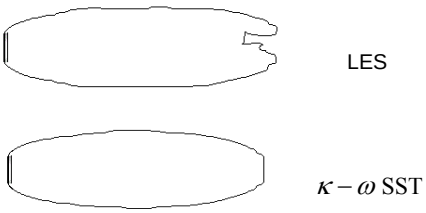

Fig. 13: Comparing the contour of vapor phase (cavity region) using two type of turbulence models, t=50 ms, $\sigma = 0.2$

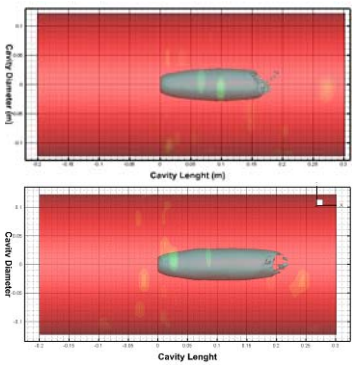

$\sigma = 0.245$

$\sigma = 0.2$

Fig. 14: Comparing the length of cavity for $\sigma = 0.245$ and $\sigma = 0.2$

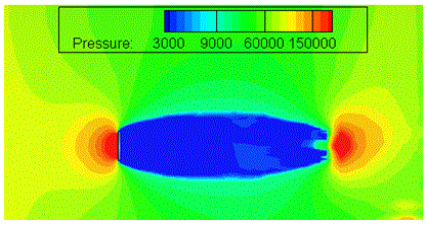

Fig. 15: Contour of pressure for $\sigma = 0.2$

Table 1: Computed parameters at $\sigma = 0.2$

Method	Simulation LES	Simulation $\kappa - \omega$ SST	Richardt's Theory [6]	Exp. [1]
L/d	8.57	8.16	5.78	7.46
D/d	2.4	2.27	2.3	2.66
C_D	1.03	1.03	1.00	1.01

Table 2: Computed parameters at $\sigma = 0.245$

Method	Simulation LES	Simulation $\kappa - \omega$ SST	Richardt's Theory [6]	Exp. [1]
L/d	6.08	5.18	4.42	5.99
D/d	2.2	2.08	2.13	2.36
C_D	1.04	1.04	1.04	1.03

References

1- Self, M. and Ripken, J. F. Steady state –cavity studies in free-jet water tunnel. St. Anthony Falls Hydrodynamic Laboratory Report 47, 1955.

2- Weller H.G. A new approach to VOF-based interface capturing methods for incompressible and compressible flow, Technical Report TR/HGW/04, OpenCFD Ltd., 2008.

3- Sauer, J. Instationaren kaviterendeStromung – Ein neues Modell, baserend auf Front Capturing (VoF) and Blasendynamik, Ph.D. Thesis, Universitat, Karlsruhe, 2000

4- Kunz, R. F., Boger, D. A., Stinebring, D. R., Chyczewski, T. S., Gibeling, H. J., Venkateswaran, S. and Govindan, T. R. A preconditioned Navier-Stokes method for two-phase flows with application to cavitation prediction. *J. Comput. Fluids*, 2000, 29, 849-875.

5- Merkle, C. L., Feng, J. Z., and Buelow, P. E. O. Computational modeling of the dynamic of sheet cavitation. *In Proceedings of the Third International Symposium on Cavitation*, Grenoble, France, 1998, pp. 307-311.

6- Passandideh-Fard, M., Roohi, E., Transient simulations of cavitating flows using a modified volume-of-fluid (VOF) technique, *International Journal of Computational Fluid Dynamics*, Volume 22, 2008, Pages 97-114.

7- Nouri N.M., Moghimi M. and Mirsaeedi S.M.H., Numerical Simulation of Unsteady Cavitating Flow Over a Disk, *Proc. IMechE*, Vol.224, 2010, pp. 1245-1253

8- Baradaran Fard, M., Nikseresht, A. H., Numerical simulation of unsteady 3D cavitating flows over axisymmetric cavitators, *Scientia Iranica, Transactions B: Mechanical Engineering*, Volume 19, 2012, Pages 1258-1264.

9- Shang, Z. Emerson, D. R. and Xiaojun Gu, Numerical investigations of cavitation around a high speed submarine using OpenFOAM with LES, *International Journal of Computational Methods*, Volume 9, 2012, 1250040-1250054.

10- Roohi, E., Zahiri, A. P., Passandideh-Fard, M., Numerical Simulation of Cavitation around a Two-Dimensional Hydrofoil Using VOF Method and LES Turbulence Model, *Applied Mathematical Modeling*, DOI: 10.1016/j.apm.2012.09.002.

11- Bensow, R. E. and Bark, G., "Simulating cavitating flows with LES in OpenFOAM" V European Conference on Computational Fluid Dynamics, pp. 14-17 June, 2010.

12- Lu, N.X., "Large Eddy Simulation of Cavitating Flow on Hydrofoils" licentiate of engineering thesis, Department of Shipping and Marine Technology, Chalmers University of Technology, Göteborg, Sweden, 2010.

13- Sagaut T, P., 2006, "Large Eddy Simulation for Incompressible Flows" Springer, New York, 3rd edition.

14- Fureby, C., and Grinstein, F., "Large Eddy Simulation of High-Reynolds Number Free and Wall-Bounded Flows" journal of Computational Physics,Vol.181, pp. 68–97, 2002.

15- Menter, F. R., Two-equation eddy-viscosity turbulence models for engineering applications, AIAA J., 1994, Volume 32, Pages 1598-1605.

16- Ubbink O., "Numerical prediction of two fluid systems with sharp interfaces" PhD thesis, Imperial College, University of London, UK, 1999.

17- Issa, R.I., "Solution of the implicitly discretized fluid flow equations by operator-splitting," Journal of Computational Physics, Vol. 62, 40–65, 1986.

18- Jasak, H., "Error analysis and estimation for the finite volume method with applications to fluid flows," PhD thesis, Imperial College of Science, Technology and Medicine, London, 1996.

19- Rusche, H., "Computational fluid dynamics of dispersed two-phase flows at high phase fractions," PhD thesis, Imperial College of Science, Technology and Medicine, London, 2002.

20- Franc, J.P. and Michel J.M., Fundamentals of Cavitation, 115 Kluwer Academic Publisher, Netherlands Section: 6 (2004)